ISSN (e): **2250 – 3005** || Volume, 08 || Issue, 1|| January – 2018 ||
International Journal of Computational Engineering Research (IJCER)

Performance Analysis of various Modulation Schemes on Inter Satellite Communication Link

[1]Vineela Kanaparthi, [2]Madhu Ramarakula
Department of Electronics and Communication Engineering
University College of Engineering Kakinada Jawaharlal Nehru Technological University Kakinada
Kakinada - 533003, India
Corresponding Author: Vineela Kanaparthi,

ABSTRACT
Global space agencies uses satellite programme to cover wide variety of areas and caters to the needs of various applications such as communication, navigation, earth observation etc. In the application of earth observation, satellites are placed in Low Earth Orbit(LEO) in order to gather high resolution data about the earth. But the visibility time of LEO satellites is in the order of minutes which are not sufficient to transmit high resolution data from LEO satellite to ground station antennas. As Geostationary Earth Orbit(GEO) satellite has high visibility time, therefore the inter satellite communication link is necessary between LEO and GEO satellites so that high resolution data gathered by LEO satellite is transferred to GEO satellite which in turn transmitted to the ground stations effectively. In this paper, the performance characteristics of the inter satellite communication link with three modulation schemes such as QPSK, 8-PSK and 16-QAM along with Saleh, Ghorbhani and Rapp amplifier models are described through Error vector magnitude(EVM) as a measuring parameter. Doppler Effect due to relative motion between LEO and GEO satellites is observed in the communication medium. It is observed that, the 16-QAM scheme provides a better EVM as compared to other modulation schemes for a given amplifier model.

Keywords: *Inter satellite communication link, Error Vector Magnitude, GEO, QPSK, 8-PSK, 16-QAM, Doppler effect*

Date of Submission: 28-12-2017 Date of acceptance: 14-01-2018

I. INTRODUCTION

The satellite programme of various space agencies are mainly organized as remote sensing, communication, navigation and scientific missions. Desires are expanding from client group for new sort of administrations like satellite connections for web accessibility on aeroplanes, data links for UAV operations. These applications require larger amount of data to be transmitted in a brief timeframe and infrequently even in genuine time. High frequency is needed as it requires greater bandwidth for transmitting large amount of data with high data rate [1]. All the above systems employing higher data rates consume high DC power available in the satellite. The satellite power is generated through solar panels and excess required power is drawn from the battery.Based on the height in which we placed the satellites, these are of three types. LEO satellite is at a height of 200 to 1200 km travel with a high velocity of 8km/sec with orbital time of 90 minutes. As these are nearer to the earth these are used for monitoring the earth with high resolution. A medium earth circle (MEO) satellite is unified with a circle inside the range from a couple of hundred miles to a couple of thousand miles over the world's surface with an orbital time of 2 to 12 hours. Global positioning system uses the medium earth orbits. A GEO satellite is an earth-circling satellite; set at a height of roughly 35,800 kilometers (22,300 miles) specifically finished the equator, which spins an indistinguishable way from the earth pivots with an orbital time of 24 hours. This is mostly used for communication purpose. Modulation is used to carry the information signal to long distances by using another signal called carrier signal. Mostly used modulations in satellite communication are Quadrature Phase Shift Keying (QPSK), 8-Phase Shift Keying (8-PSK), 16-Quadrature Amplitude Modulation (16-QAM). These are used for carrying more information in less bandwidth so that we are able to transmit high resolution data with in less time[2].In this paper, the effects of different modulation schemes along with different amplifier models are observed in the transmitter section of LEO-GEO inter satellite communication link through constellation diagrams and measure the performance in terms of EVM value. Channel impairments like Doppler Effect are observed by varying the Doppler frequency values and in each case EVM values are noted. In receiver section, thermal noise effect, mismatching in I and Q channels effect are observed on the link performance. This inter satellite communication link is used in the realization of data transmission systems of inter satellite link like Tracking and Data Relay Systems (TDRSS) made by NASA, KODAMA made by Japan and European data relay satellite systems (EDRSS)[3].

II. INTER SATELLITE COMMUNICATION

The remote sensing satellites are low earth orbiting satellites which transmit data to ground stations during the visibility time. The visibility times are usually of the orders of 15-20 minutes. The ground stations have to track and acquire the data from remote sensing satellites. With the limitation on visibility times on ground station antennas for good RF links, the limitation on amount of data and data rates arises for LEO satellites in the currently used bands[4].Because of the coming of higher determination satellites, the information and information rates are likewise high[5]. On the off chance that vast determination information is to be transmitted with confinements on perceivability times, size of installed memory module and ground station following and availability, the need of entomb satellite correspondence connect between LEO-GEO satellite emerges and subsequently the requirement for higher recurrence groups to help higher information rates.
The block diagram representing the inter satellite communication link is as shown in below Figure 1.

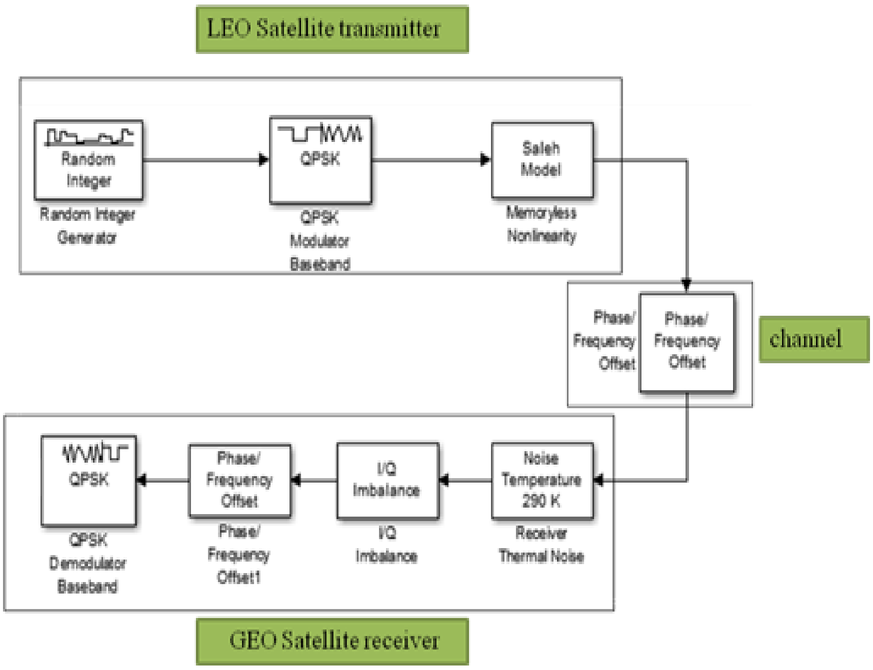

Figure 1.Block diagram of inter satellite communication link

2.1. Random generator block

It generates the data which is nothing but high resolution data gathered from the earth by LEO satellite.

2.2. Modulation Techniques

The performance of three modulation techniques such as QPSK, 8-PSK, 16-QAM on inter satellite communication link are observed.

2.2.1.QPSK

It is a digital modulation technique in which we consider two bits as a symbol and assigning a one of the four phases to a particular symbol[6] [8]. The QPSK modulated signal is given by

$$Y(t) = \sqrt{\frac{2E_s}{T}} \cos\left(2\pi f_c t + (2n-1)\frac{\pi}{4}\right) \quad (1)$$

where, E_s = Symbol energy, T = Symbol period, f_c = Carrier frequency and n = 1,2,3,4.

2.2.2.8-PSK

In which we take three bits at a time and modulating by assigning one of the eight phases with each phase separated by a $\pi/8$. 8-PSK modulated signal[7]

$$Y(t) = \sqrt{\frac{2E_s}{T}} \cos\left(2\pi f_c t + (2n-1)\frac{\pi}{8}\right) \qquad (2)$$

2.2.3.16-QAM

It is a modulation technique in which the information stored in the form of both amplitude and phase of a carrier signal so that increases the receiver sensitivity in the detection process. QAM has the advantage of using two signal frequencies which are shifted by 90°. Here the input binary data is split into four channels namely I, I', Q, Q'. Where I, Q bits gives sign of the output at 2 to 4 level converters and I', Q' determine the magnitude of the output. The minimum bandwidth required is $f_b/4$, where f_b is frequency of a bit.QAM signal is[9].

$$\text{Y(t)} = A_c\left(a_{In} + ja_{Qn}\right)e^{(2\pi f_c t + \theta_c)} \qquad (3)$$

where, $a_{In} =$ in phase component amplitude, $a_{Qn} =$ quadrature phase component amplitude and $\theta_c =$ phase of carrier signal.

2.3. Amplifier models

Generally amplifier means it will strengthen the signal i.e., it will increase the amplitude of the signal. But practically amplifier produce amplification up to certain level of input voltage value after that value it will produce less amplification and also gives phase distortion along with amplification. Amplifiers used in the satellite are modeled by three scientists namely Saleh, Ghorbani and Rapp[10].

2.3.1.Saleh amplifier model

The Saleh model is a quasi memory-less model. In this model in order to fit the model to measurement data four parameters are needed[12].

Its AM-AM conversion function is

$$A(m) = \frac{\alpha_a m}{1 + \beta_a m^2} \qquad (4)$$

Its AM-PM conversion function is

$$P(m) = \frac{\alpha_p m^2}{1 + \beta_p m^2} \qquad (5)$$

where, $\alpha_a, \beta_a, \alpha_p, \beta_p$ are the demonstrate parameters and *m* is the amplitude of the input signal.

2.3.2.Ghorbani amplifier model

The Ghorbani model utilizes eight parameters to fit the model to the estimation information; this model is semi memory-less. It's AM-AM conversion function is[13].

$$A(m) = \frac{r_1 m^{r_2}}{1 + r_3 m^{r_2}} + r_4 m \qquad (6)$$

Its AM-PM conversion function is

$$P(m) = \frac{s_1 m^{s_2}}{1 + s_3 m^{s_2}} + s_4 m \qquad (7)$$

where, $r_1, r_2, r_3, r_4, s_1, s_2, s_3, s_4$ the parameters of this model and *m* is the signal amplitude.

2.3.3.Rapp amplifier model

The Rapp model utilizes three parameters, and it experiences amplitude distortion but no phase distortion. The general expression of the AM-AM conversions is as follows [14],

$$A(m) = \frac{m}{\left[1 + \left(\frac{m}{O_{sat}}\right)^{2S}\right]^{\frac{1}{2S}}} \qquad (8)$$

where, O_{sat} is a parameter that sets the yield immersion level and *S* is a parameter that sets the smoothness of the progress from straight to immersion states. Smaller *s* value demonstrates smooth change.

2.4.Doppler effect

This is the change in frequency due to the relative movement exists between two bodies. Here both LEO and GEO satellite are rotating around the earth with different velocities. So Doppler frequency related to original frequency is as follows[15].

$$f_d = f_c * \frac{v}{c} \qquad (9)$$

where, f_d = Doppler frequency, f_c = carrier frequency, v = velocity of transmitted wave and c = velocity of light.

2.5.Thermal noise

It is an electronic disturbance produced due to thermal effect of charge carriers within an electronic device regardless of applied voltage. All this related to the device in the receiver section. We take the thermal noise in the form of noise figure as

$$Noise\ Figure = 10 * \log_{10}\left(1 + \frac{noise\ temparature}{290}\right) \qquad (10)$$

Noise figure is nothing but decibel equivalent of noise factor.

2.6.I/Q Imbalance

It is one of the execution restricting elements in the designing of direct transformation receivers. I/Q imbalance are nothing but the existing of mismatches in the in-phase and out-phase of a receiving section.

2.7.Error vector magnitude(EVM)

EVM is an efficient technique used in determining performance of cellular communication systems. It is measure of standard deviation of the points about an average value of a constellation point[16]. EVM allows us to test the quality of the modulated signal/symbol. Equation of EVM for calculating the error measurement between ideal constellation and received constellation in percentage is

$$EVM = \sqrt{\frac{\frac{1}{N}\sum_{j=1}^{N} e_j}{\frac{1}{N}\sum_{j=1}^{N}\left(I_j^2 + Q_j^2\right)}} \qquad (11)$$

where, $$e_j = \left(I_j - I_j^1\right)^2 + \left(Q_j - Q_j^1\right)^2 \qquad (12)$$

I_j, Q_j are the in-phase and quadrature phase components of a ideal constellation. I_j', Q_j' are the in-phase and quadrature-phase components of a received constellation.

III. MATHEMATICAL ANALYSIS

QPSK with Saleh model:

QPSK modulated signal $= A_c \cos\left(2\pi f_c t + (2n-1)\frac{\pi}{4}\right)$

For n=1, QPSK modulated signal = $A_c \cos\left(2\pi f_c t + \frac{\pi}{4}\right)$

In Saleh model

AM-AM conversion is, $A(r) = \frac{\alpha_A r}{1 + \beta_A r^2}$

AM-PM conversion is, $\phi(r) = \frac{\alpha_P r^2}{1 + \beta_P r^2}$,

Distorted signal after amplifier modeled by the Saleh model is $= A(r)\cos\left(2\pi f_c t + \frac{\pi}{4} + \phi(r)\right)$

Consider $\alpha_A = 2.1587$, $\beta_A = 1.1517$, $\alpha_P = 4.0033$, $\beta_P = 9.1040$

$$= \frac{2.1587 A_c}{1 + (1.1517) A_c^2} \cos\left(2\pi f_c t + \frac{\pi}{4} + \frac{(4.033) A_c^2}{1 + (9.1040) A_c^2}\right)$$

$$= \frac{2.1587 A_c}{1 + (1.1517) A_c^2} \left\{ \cos\left(\frac{\pi}{4} + \frac{(4.033) A_c^2}{1 + (9.1040) A_c^2}\right) \cos 2\pi f_c t - \sin\left(\frac{\pi}{4} + \frac{(4.033) A_c^2}{1 + (9.1040) A_c^2}\right) \sin 2\pi f_c t \right\}$$

After Doppler Effect the signal becomes

$$= \frac{2.1587A_c}{1+(1.1517)A_c^2}\cos\left(2\pi(f_c+f_d)t+\frac{\pi}{4}+\frac{(4.033)A_c^2}{1+(9.1040)A_c^2}\right)$$

The amplitude of above signal is

$$= \frac{2.1587\ A_c}{1+(1.1517\ )A_c^2}\sqrt{\cos^2\left(2\pi f_d t+\frac{\pi}{4}+\frac{(4.033\ )A_c^2}{1+(9.1040\ )A_c^2}\right)+\sin^2\left(2\pi f_d t+\frac{\pi}{4}+\frac{(4.033\ )A_c^2}{1+(9.1040\ )A_c^2}\right)}$$

$$= \frac{2.1587\ A_c}{1+(1.1517\ )A_c^2}$$

From the above equation it is clearly shows that there is no amplitude distortion occurred after the Doppler Effect. Phase of the above signal is

$$= \tan^{-1}\left\{\frac{\sin\left(2\pi f_d t+\frac{\pi}{4}+\frac{(4.033)A_c^2}{1+(9.1040)A_c^2}\right)}{\cos\left(2\pi f_d t+\frac{\pi}{4}+\frac{(4.033)A_c^2}{1+(9.1040)A_c^2}\right)}\right\}$$

$$= \tan^{-1}\left\{\tan\left(2\pi f_d t+\frac{\pi}{4}+\frac{(4.033)A_c^2}{1+(9.1040)A_c^2}\right)\right\}$$

$$= 2\pi f_d t+\frac{\pi}{4}+\frac{(4.033)A_c^2}{1+(9.1040)A_c^2}$$

From the above equation it is clearly shows that additional phase distortion produced to the amplifier phase distortion in the form of $2\pi f_d t$ due to Doppler Effect.

3.1.EVM calculations

EVM value for QPSK modulation after Saleh model amplifier*:*

$$\text{EVM} = \sqrt{\frac{\frac{1}{N}\sum_{k=1}^{N} e_k}{\frac{1}{N}\sum_{k=1}^{N}\left(I_k^2+Q_k^2\right)}}\times 100, \quad \text{Where } e_k = \left(I_k - I_k^{'}\right)^2 + \left(Q_k - Q_k^{'}\right)^2$$

QPSK modulated signal = $A_c \cos\left(2\pi f_c t + (2n-1)\frac{\pi}{4}\right)$

For n=1, $= \frac{A_c}{\sqrt{2}}\cos 2\pi f_c t - \frac{A_c}{\sqrt{2}}\sin 2\pi f_c t$

$$I_1 = \frac{A_c}{\sqrt{2}}, Q_1 = -\frac{A_c}{\sqrt{2}}$$

After Saleh model amplifier, it becomes $= \frac{\alpha_A A_c}{1+\beta_A A_c^2}\cos\left(2\pi f_c t+\frac{\pi}{4}+\frac{\alpha_P A_c^2}{1+\beta_P^2}\right)$

$$I_1^{'} = \frac{\alpha_A A_c}{1+\beta_A A_c^2}\cos\left(\frac{\pi}{4}+\frac{\alpha_P A_c^2}{1+\beta_P A_c^2}\right),\ Q_1^{'} = -\frac{\alpha_A A_c}{1+\beta_A A_c^2}\sin\left(\frac{\pi}{4}+\frac{\alpha_P A_c^2}{1+\beta_P^2}\right)$$

$$e_1 = \left\{\frac{A_c}{\sqrt{2}} - \frac{\alpha_A A_c}{1+\beta_A A_c^2}\cos\left(\frac{\pi}{4}+\frac{\alpha_P A_c^2}{1+\beta_P A_c^2}\right)\right\}^2 + \left\{-\frac{A_c}{\sqrt{2}} + \frac{\alpha_A A_c^2}{1+\beta_A A_c^2}\cos\left(\frac{\pi}{4}+\frac{\alpha_P A_c^2}{1+\beta_P A_c^2}\right)\right\}^2$$

$$= A_c^2 + \left(\frac{\alpha_A A_c}{1+\beta_A A_c^2}\right)^2 - \frac{2\alpha_A A_c^2}{1+\beta_A A_c^2}\cos\left(\frac{\alpha_P A_c^2}{1+\beta_P A_c^2}\right)$$

$$e_2 = \left(I_2 - I_2^{'}\right)^2 + \left(Q_2 - Q_2^{'}\right)^2$$

$$I_2 = -\frac{A_c}{\sqrt{2}},\ Q_2 = -\frac{A_c}{\sqrt{2}}$$

$$I_2^{'} = \frac{\alpha_A A_c}{1+\beta_A A_c^2}\cos\left(\frac{3\pi}{4}+\frac{\alpha_P A_c^2}{1+\beta_P A_c^2}\right),\ Q_2^{'} = -\frac{\alpha_A A_c}{1+\beta_A A_c^2}\sin\left(\frac{3\pi}{4}+\frac{\alpha_P A_c^2}{1+\beta_P A_c^2}\right)$$

$$= \left\{-\frac{A_c}{\sqrt{2}} - \frac{\alpha_A A_c}{1+\beta_A A_c^2}\cos\left(\frac{3\pi}{4}+\frac{\alpha_P A_c^2}{1+\beta_P A_c^2}\right)\right\}^2 + \left\{-\frac{A_c}{\sqrt{2}} + \frac{\alpha_A A_c^2}{1+\beta_A A_c^2}\sin\left(\frac{3\pi}{4}+\frac{\alpha_P A_c^2}{1+\beta_P A_c^2}\right)\right\}^2$$

$$= A_c^2 + \left(\frac{\alpha_A A_c}{1+\beta_A A_c^2}\right)^2 - \frac{2\alpha_A A_c^2}{1+\beta_A A_c^2}\left[\cos\left(\frac{3\pi}{4}+\frac{\alpha_P A_c^2}{1+\beta_P A_c^2}\right) - \sin\left(\frac{3\pi}{4}+\frac{\alpha_P A_c^2}{1+\beta_P A_c^2}\right)\right]$$

$$= A_c^2 + \left(\frac{\alpha_A A_c}{1+\beta_A A_c^2}\right)^2 - \frac{2\alpha_A A_c^2}{1+\beta_A A_c^2}\cos\left(\frac{\alpha_P A_c^2}{1+\beta_P A_c^2}\right)$$

$$e_3 = \left(I_3 - I_3^1\right)^2 + \left(Q_3 - Q_3^{'}\right)^2$$

$$I_3 = -\frac{A_c}{\sqrt{2}},\ Q_3 = \frac{A_c}{\sqrt{2}}$$

$$= \left\{-\frac{A_c}{\sqrt{2}} - \frac{\alpha_A A_c}{1+\beta_A A_c^2}\cos\left(\frac{5\pi}{4}+\frac{\alpha_P A_c^2}{1+\beta_P A_c^2}\right)\right\}^2 + \left\{\frac{A_c}{\sqrt{2}} + \frac{\alpha_A A_c}{1+\beta_A A_c^2}\sin\left(\frac{5\pi}{4}+\frac{\alpha_P A_c^2}{1+\beta_P A_c^2}\right)\right\}^2$$

$$= A_c^2 + \left(\frac{\alpha_A A_c}{1+\beta_A A_c^2}\right)^2 + \frac{\sqrt{2}\alpha_A A_c^2}{1+\beta_A A_c^2}\left\{\cos\left(\frac{5\pi}{4}+\frac{\alpha_P A_c^2}{1+\beta_P A_c^2}\right) + \sin\left(\frac{5\pi}{4}+\frac{\alpha_P A_c^2}{1+\beta_P A_c^2}\right)\right\}$$

$$= A_c^2 + \left(\frac{\alpha_A A_c}{1+\beta_A A_c^2}\right)^2 - \frac{2\alpha_A A_c^2}{1+\beta_A A_c^2}\cos\left(\frac{\alpha_P A_c^2}{1+\beta_P A_c^2}\right)$$

$$e_4 = \left(I_4 - I_4^{'}\right)^2 + \left(Q_4 - Q_4^{'}\right)^2$$

Modulated signal $= A_c\cos\left(2\pi f_c t + \frac{7\pi}{4}\right)$

$$= \left\{\frac{A_c}{\sqrt{2}} - \frac{\alpha_A A_c}{1+\beta_A A_c^2}\cos\left(\frac{7\pi}{4}+\frac{\alpha_P A_c^2}{1+\beta_P A_c^2}\right)\right\}^2 + \left\{\frac{A_c}{\sqrt{2}} + \frac{\alpha_A A_c}{1+\beta_A A_c^2}\sin\left(\frac{7\pi}{4}+\frac{\alpha_P A_c^2}{1+\beta_P A_c^2}\right)\right\}$$

$$= A_c^2 + \frac{\alpha_A A_c}{1+\beta_A A_c^2} - \frac{\sqrt{2}\alpha_A A_c^2}{1+\beta_A A_c^2}\left(\cos\left(\frac{7\pi}{4}+\frac{\alpha_P A_c^2}{1+\beta_P A_c^2}\right) - \sin\left(\frac{7\pi}{4}+\frac{\alpha_P A_c^2}{1+\beta_P A_c^2}\right)\right)$$

$$\sum_{k=1}^{4} e_k = e_1 + e_2 + e_3 + e_4$$

$$= 4A_c^2 + 4\left(\frac{\alpha_A A_c}{1+\beta_A A_c^2}\right)^2 - 8\frac{\alpha_A A_c^2}{1+\beta_A A_c^2}\cos\left(\frac{\alpha_P A_c^2}{1+\beta_P A_c^2}\right)$$

$$\text{EVM} = \sqrt{\frac{\frac{1}{N}\sum_{k=1}^{N} e_k}{\frac{1}{N}\sum_{k=1}^{N}\left(I_k^2 + Q_k^2\right)}} \times 100$$

$$=\sqrt{\frac{4A_c^2+4\left(\frac{\alpha_A A_c}{1+\beta_A A_c^2}\right)^2-\frac{8\alpha_A A_c^2}{1+\beta_A A_c^2}\cos\left(\frac{\alpha_P A_c^2}{1+\beta_P A_c^2}\right)}{4A_c^2}}\times 100$$

$$=\sqrt{1+\left(\frac{\alpha_A}{1+\beta_A A_c^2}\right)^2-\frac{2\alpha_A}{1+\beta_A A_c^2}\cos\left(\frac{\alpha_P A_c^2}{1+\beta_P A_c^2}\right)}\times 100$$

EVM value for QPSK modulation after Doppler effect*:*

Modulated signal = $A_c\cos\left(2\pi f_c t+(2n-1)\frac{\pi}{4}\right)$ n=1,2,3,4

After Saleh model amplifier $=\frac{A_c\alpha_A}{1+\beta_A A_c^2}\cos\left(2\pi f_c t+(2n-1)\frac{\pi}{4}+\frac{\alpha_P A_c^2}{1+\beta_p A_c^2}\right)$

After Doppler effect this signal becomes

$$=\frac{A_c\alpha_A}{1+\beta_A A_c^2}\cos\left(2\pi(f_c+f_d)t+(2n-1)\frac{\pi}{4}+\frac{\alpha_P A_c^2}{1+\beta_P A_c^2}\right)$$

EVM

$$e_k=(I_k-I_k^{'})^2+(Q_k-Q_k^{'})^2$$

$$e_1=(I_1-I_1^{'})^2+(Q_1-Q_1^{'})^2$$

$$=\left\{\frac{A_c}{\sqrt{2}}-\frac{\alpha_A A_c}{1+\beta_A A_c^2}\cos\left(2\pi f_d t+\frac{\pi}{4}+\frac{\alpha_A A_c^2}{1+\beta_P A_c^2}\right)\right\}^2+\left\{\frac{A_c}{\sqrt{2}}+\frac{\alpha_A A_c}{1+\beta_A A_c^2}\sin\left(2\pi f_d t+\frac{\pi}{4}+\frac{\alpha_P A_c^2}{1+\beta_P A_c^2}\right)\right\}^2$$

$$=A_c^2+\left(\frac{\alpha_A A_c}{1+\beta_A A_c^2}\right)^2-\frac{2\alpha_A A_c^2}{1+\beta_A A_c^2}\cos\left(2\pi f_d t+\frac{\alpha_P A_c^2}{1+\beta_P A_c^2}\right)$$

$$e_2=(I_2-I_2^{'})^2+(Q_2-Q_2^{'})^2$$

$$=\left\{-\frac{A_c}{\sqrt{2}}-\frac{\alpha_A A_c}{1+\beta_A A_c^2}\cos\left(2\pi f_d t+\frac{3\pi}{4}+\frac{\alpha_A A_c^2}{1+\beta_P A_c^2}\right)\right\}^2+\left\{-\frac{A_c}{\sqrt{2}}+\frac{\alpha_A A_c}{1+\beta_A A_c^2}\sin\left(2\pi f_d t+\frac{3\pi}{4}+\frac{\alpha_P A_c^2}{1+\beta_P A_c^2}\right)\right\}^2$$

$$=A_c^2+\left(\frac{\alpha_A A_c}{1+\beta_A A_c^2}\right)^2-\frac{2\alpha_A A_c^2}{1+\beta_A A_c^2}\cos\left(2\pi f_d t+\frac{\alpha_P A_c^2}{1+\beta_P A_c^2}\right)$$

$$e_3=(I_3-I_3^{'})^2+(Q_3-Q_3^{'})^2$$

$$=\left\{-\frac{A_c}{\sqrt{2}}-\frac{\alpha_A A_c}{1+\beta_A A_c^2}\cos\left(2\pi f_d t+\frac{5\pi}{4}+\frac{\alpha_A A_c^2}{1+\beta_P A_c^2}\right)\right\}^2+\left\{\frac{A_c}{\sqrt{2}}+\frac{\alpha_A A_c}{1+\beta_A A_c^2}\sin\left(2\pi f_d t+\frac{5\pi}{4}+\frac{\alpha_P A_c^2}{1+\beta_P A_c^2}\right)\right\}^2$$

$$=A_c^2+\left(\frac{\alpha_A A_c}{1+\beta_A A_c^2}\right)^2-\frac{2\alpha_A A_c^2}{1+\beta_A A_c^2}\cos\left(2\pi f_d t+\frac{\alpha_P A_c^2}{1+\beta_P A_c^2}\right)$$

$$e_4=(I_4-I_4^{'})^2+(Q_4-Q_4^{'})^2$$

$$=\left\{\frac{A_c}{\sqrt{2}}-\frac{\alpha_A A_c}{1+\beta_A A_c^2}\cos\left(2\pi f_d t+\frac{7\pi}{4}+\frac{\alpha_A A_c^2}{1+\beta_P A_c^2}\right)\right\}^2+\left\{\frac{A_c}{\sqrt{2}}+\frac{\alpha_A A_c}{1+\beta_A A_c^2}\sin\left(2\pi f_d t+\frac{7\pi}{4}+\frac{\alpha_P A_c^2}{1+\beta_P A_c^2}\right)\right\}^2$$

$$= A_c^2 + \left(\frac{\alpha_A A_c}{1+\beta_A A_c^2}\right)^2 - \frac{2\alpha_A A_c^2}{1+\beta_A A_c^2}\cos\left(2\pi f_d t + \frac{\alpha_P A_c^2}{1+\beta_P A_c^2}\right)$$

$$EVM = \sqrt{\frac{4A_c^2 + 4\left(\frac{\alpha_A A_c}{1+\beta_A A_c^2}\right)^2 - \frac{8\alpha_A A_c^2}{1+\beta_A A_c^2}\cos\left(2\pi f_d t + \frac{\alpha_P A_c^2}{1+\beta_P A_c^2}\right)}{4A_c^2}} \times 100$$

$$= \sqrt{1 + \left(\frac{\alpha_A}{1+\beta_A A_c^2}\right)^2 - \frac{2\alpha_A}{1+\beta_A A_c^2}\cos\left(2\pi f_d t + \frac{\alpha_P A_c^2}{1+\beta_P A_c^2}\right)} \times 100$$

IV. RESULTS AND DISCUSSION

Constellation diagram is a graphical representation of a signal components modulated by a digital modulation scheme. It displays the signal as a two-dimensional scatter diagram in the complex plane[17].

4.1.QPSK modulation:

The constellation diagrams for QPSK modulated signal at different stages in a link with Saleh model amplifier are shown in Figure 2.

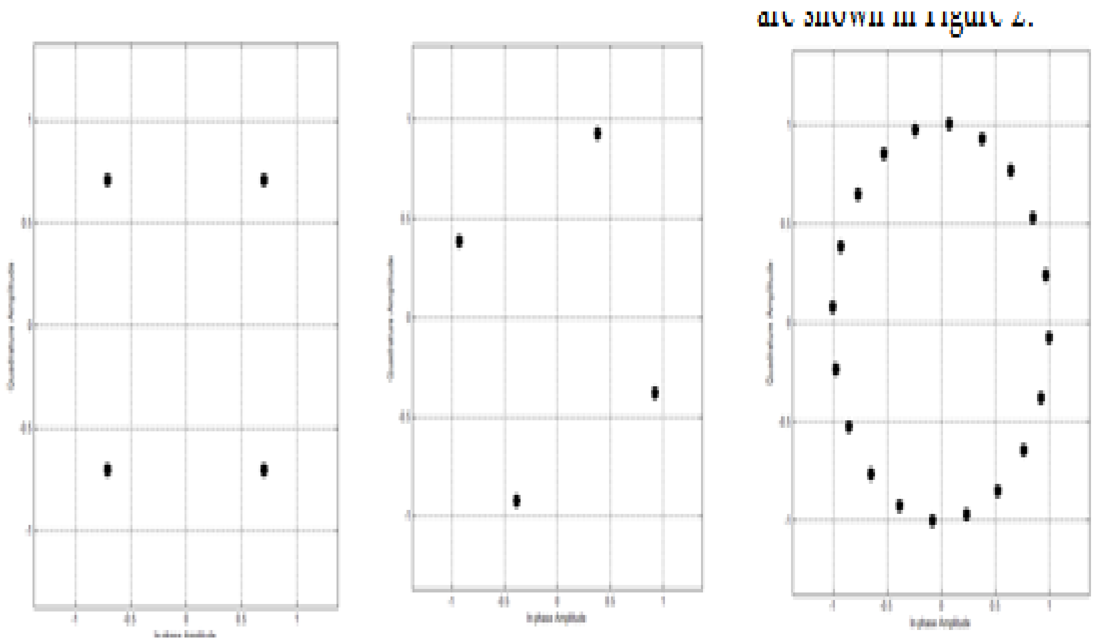

(i) Basic constellation (ii) After Saleh model amplifier (iii) After Doppler effect

Figure 2. QPSK Constellation diagrams

QPSK uses four phases to represent the information, so its constellation consisting of 4 points as shown in Figure 2(i). It is distorted both in amplitude and phase by Saleh model amplifier which is shown in Figure 2(ii) and Doppler Effect is observed to the Saleh model distorted signal in the Figure 2(iii).

The EVM values are noted for different Doppler frequencies for QPSK modulation, which is shown in Figure 3.

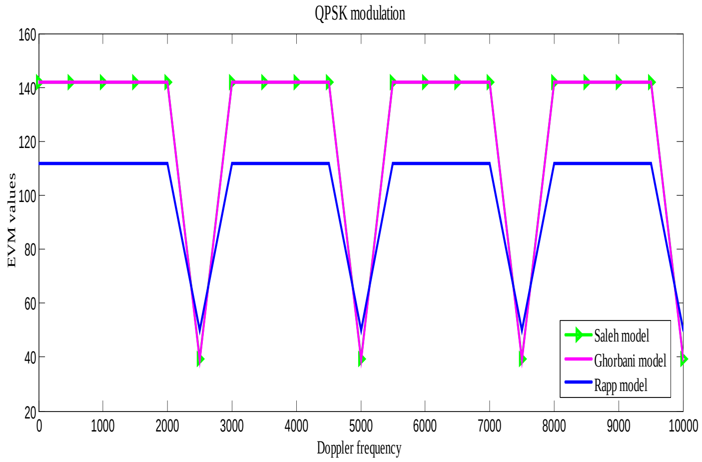

Figure 3. EVM values versus **D**oppler frequency of QPSK modulation

At Doppler frequency of 2500Hz and its multiples, EVM value produced is same as the value at the corresponding amplifier. For remaining frequencies its EVM value is greater and different.

4.2. 8-PSK:

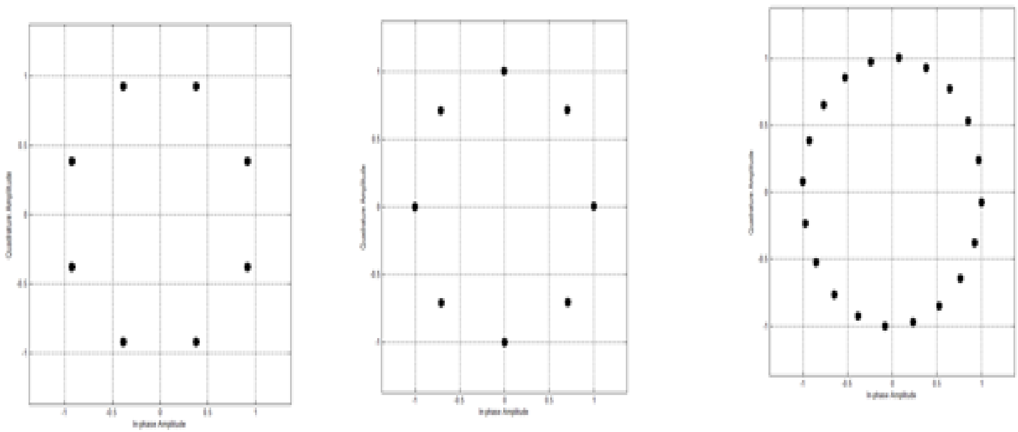

(i) Basic constellation (ii) After saleh model amplifier (iii) After doppler effect

Figure 4. 8-PSK modulation

8-PSK modulation assigns eight phases to the information bits, so its constellation has eight points as shown in Figure 4(i). The effect of amplifier to this constellation is observed in Figure 4(ii). The Figure 4(iii) shows the Doppler Effect to the amplifier distorted signal.The EVM values are noted for different Doppler frequencies for 8-PSK modulation, which is shown in Figure 5.

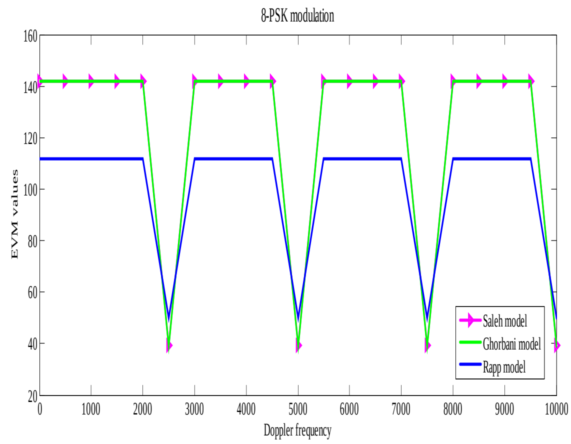

Figure 5. EVM values versus Doppler frequency of 8-PSK modulation

In this there is no Doppler effect at the frequency of 2500Hz and its harmonics, for remaining Doppler frequencies EVM value is constant and higher.

4.3. 16-QAM:

The constellation diagrams for 16-QAM modulated signal at different stages in a link are as shown in Figure 6.

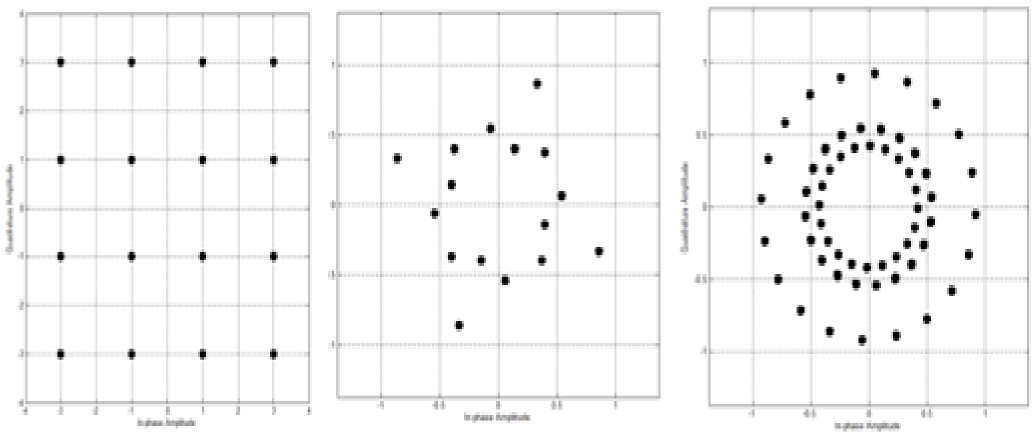

(i) Basic constellation (ii) After saleh model amplifier (iii) After doppler effect

Figure 6. 16-QAM modulation

This modulation produces16 constellation points by varying 4 amplitudes and four phases, which is shown in Figure 6(i). Amplifier distortion to this constellation is observed in Figure 6(ii) and Doppler Effect is observedin the Figure 6(iii). The EVM values are noted for different Doppler frequencies for 16-QAM, which is shown in Figure 7.

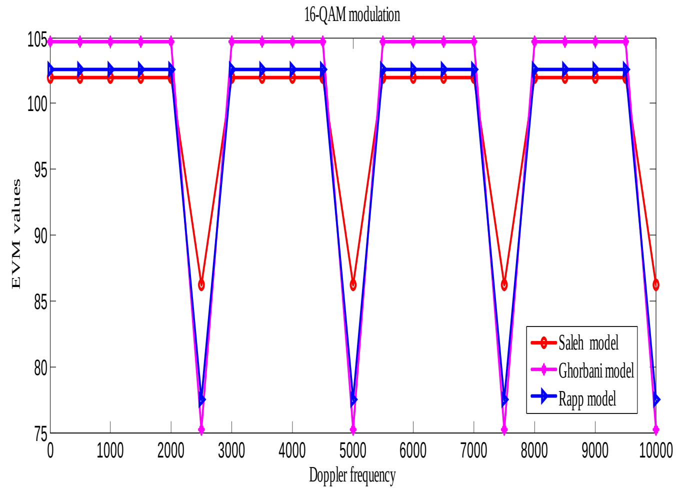

Figure 7. EVM values versus Doppler frequency of 16-QAM modulation

In 16-QAM modulation also there is no Doppler effect at frequencies of 2500Hz and its multiples for three amplifier models; at remaining frequencies EVM value is constant.

V. EVM ANALYSIS

The EVM Values for different modulations with three amplifier models is listed in Table 1,Table 2,Table 3.

5.1.QPSK modulation

Table 1.EVM values for QPSK modulation

Parameter	EVM values		
	Saleh Model	**Ghorbani Model**	**Rapp Model**
After amplifier	39.43	38.85	50
After frequency offset	141.7	141.9	111.8
After noise figure of 3dB	141.7	141.9	111.8
After I/Q imbalance	145.4	145.7	113

5.2.8-PSK modulation

Table 2.EVM values for 8-PSK modulation

Parameter	EVM values		
	Saleh Model	**Ghorbani Model**	**Rapp Model**
After amplifier	39.43	38.85	50
After frequency offset	141.7	141.9	111.8
After noise figure of 3dB	141.7	141.9	111.8
After I/Q imbalance	145.3	145.5	112.9

5.3.16-QAM modulation

Table 3.EVM values for 16-QAM modulation

Parameter	EVM values		
	Saleh Model	**Ghorbani Model**	**Rapp Model**
After amplifier	86.26	75.25	77.51
After frequency offset	102	104.6	102.6
After noise figure of 3dB	102	104.6	102.6
After I/Q imbalance	102.2	105.1	102.8

From the above values in the tables, it is known that higher modulation i.e., 16-QAM signal experienced less distortion after passing through the different impairments such as amplifier distortion, Doppler effect, thermal noise and I/Q imbalance stages. Even though it seems to be 16-QAM is more advantage, remaining modulations are also used in inter satellite communication link in different applications.

VI. CONCLUSION

In this paper, the performance of various modulation schemes for inter satellite communication link between LEO and GEO satellites is presented. The analysis is carried out with the EVM as the important parameter with three amplifier models. For a better transceiver system, the EVM should be as low as possible. The effect of relative motion between LEO and GEO satellites i.e., Doppler Effect has also observed as a channel impairment. It is observed that, the 16-QAM given a low EVM. The EVM observed for 16-QAM with a Saleh model amplifier is105.1, whereas for QPSK and 8-PSK is 145.7 and 145.5 respectively.

REFERENCES

[1]. R. Radhakrishnan, W. W. Edmonson, F. Afghah, J. Chenou, R. M. Rodriguez-Osorio, and Q. A. Zeng, “Optimal Multiple Access Protocol for Inter-satellite Communication in Small Satellite Systems,” in The 4S Symposium, Majorca, Spain, 2014.

[2]. F. Pinto, F. Afghah, R. Radhakrishnan, and W. W. Edmonson, “Software Defined Radio Implementation of DS-CDMA in Inter-Satellite Communications for Small Satellites,” in International Conference on wireless for Space and Extreme Environments, Orlando, Florida, USA, 2015.

[3]. B. W. Barbee and et al., “Guidance and Navigation for Rendezvous and Proximity Operations with a Non-Cooperative Spacecraft at Geosynchronous Orbit,” in George H. Born Symposium, Boulder, Colorado, 2010.

[4]. “Performance analysis of Turbo coded APSK Modulations over Non –linear Satellite Channels “ Riccardo De Gaudenzi,Albert GuillenI Fabregas,and Alfonso Martinez, in IEEE transactions on Wireless Communications”, Vol no 5,No:9 September 2006 .

[5]. “Modeling of the simultaneous influence of the thermal noise and the phase noise in Space communication systems “, O Baran ,M.kasal International journal Radio engineering, 2010,Vol No 19,No:4, PP 618-626,ISSN:1210-2512.

[6]. “Capacity Analysis and System optimization for the forward link of multi-beam satellite broadband systems exploiting adaptive coding an modulation“, R.Rinaldo and R.D Gaudenzi in International Journal of satellite coomunication and Networking No :22 PP 401-423,2004.

[7]. “M-ary PSK over Non-linear Satellite Channels “, James Cladwell and clark Robertson ,PP :23 in IEEE conference PACRIM 2009. SSC02-IV-6 -16th Annual AIAA/USU Conference on SmallSatellites, Logan, Utah, USA, 2002.

[8]. B. Palmintier, C. Kitts, and M. Swartwout, \Distributed Computing Architecture for Small Satel-lite and Multi-Spacecraft Missions," in SSC02-IV-6 -16th Annual AIAA/USU Conference on SmallSatellites, Logan, Utah, USA, 2002.

[9]. C. Frmeaux, X. Pea, and J. Fourcade, \ESSAIM Cluster Disposal:Orbit Management," in SpaceOps Conference, Stockholm, Sweden, 2012.

[10]. M. Rajanna, H. C. Kantharaju, and M. G. Shiva, Satellite Networks Routing Protocol Issues and Challenges: A Survey," International Journal of Innovative Research in Computer and Communication Engineering, vol. 2, no. 2, pp. 153{157, May 2014.

[11]. D.-Y. Zhang, S. Liu, and M. li Yin, \A Satellite Routing Algorithm Based on Optimization of Both Delay and Bandwidth," in Wireless Communications, Networking and Mobile Computing (WiCOM), 2011 7th International Conference on, Sept 2011.

[12]. R. Sun, D. Maessen, J. Guo, and et al., \Enabling Inter-satellite Communication and Ranging for Small Satellites," in Proceedings of the small satellite systems and services symposium, Funchal, Portugal, 2010.

[13]. W. Guoqiang, Y. Bai, and Z. Sun, \Research on Formation of Microsatellite Communication with Genetic Algorithm," The Scientific World Journal, vol. 2013, pp. 1-7, 2013.

[14]. A. A. Atayero, M. K. Luka, and A. A. Alatishe, \Satellite Link Design: A Tutorial," International Journal of Electrical and Computer Sciences IJECS-IJENS, vol. 11, , Aug 2011.

[15]. P. Petropoulou, E. Michailidis, A. Panagopoulos, and A. Kanatas, \Radio Propagation Channel Mea-surements for Multi-Antenna Satellite Communication Systems: A Survey," Antennas and PropagationMagazine, IEEE, vol. 56, no. 6, Dec 2014.

[16]. P. Arapoglou, K. Liolis, M. Bertinelli, A. Panagopoulos, P. Cottis, and R. De Gaudenzi, Mimo over satellite: A review," Communications Surveys Tutorials, IEEE, vol. 13, no. 1, First 2011.

[17]. Alasady H., Boutros R. and Ibnkahla M."Comparison Between Digital & Analog Predistortion"Proc.IEEE. CCEC. Conference-Montreal - QB -Canada, May 2003.

[18]. Craig J. W., "A new, simple and exact result for calculating the probability of error for two-dimensional signal constellations", MILCOM proceedings, 1991, pp.571-575.

[19]. Goldsmith A. J. and Chua S. G., "Variable-Rate Variable-Power MQAM for Fading Channels" IEEE Trans. Comm. Vol.45, NO.lO, pp.1218-1231,Oct.1997.

[20]. M. Ibnkahla, Q. Rahman, A. Sulyman, H. AI-Asady, Y. Jun, and A. Safwat, "High speed satellite mobile communications: Technologies and challenges", The Proceedings of The IEEE, Special issue on Gigabit wireless communications: Technologies and challenges, pp. 312-339, February 2004.

Aslı AKSOY1. "An Integrated Model For Sourcing Strategies In Global Outsourcing." International Journal of Computational Engineering Research (IJCER), vol. 08, no. 1, 2018, pp. 01–12.